

# 5 Kinetic Investigation of Aminolysis Reaction

## 5.1 Background

### 5.1.1 Overview

The carbene carbon of Fischer type carbene complexes is electrophilic in nature<sup>[1]</sup> and undergoes facile substitution of the alkoxy group with nucleophiles such as OH<sup>-</sup>, water, MeO<sup>-</sup>, amines, thiolate ions, carbanion and others<sup>[2-19]</sup>.

The first extensive kinetic investigation of the aminolysis of alkoxy carbene complexes was carried out by Werner and Fischer<sup>[9]</sup>. They studied the reaction of [Cr(CO)<sub>5</sub>{C(OMe)Ph}] with the primary amines RNH<sub>2</sub> (R = *n*-C<sub>4</sub>H<sub>9</sub>, C<sub>6</sub>H<sub>11</sub>, CH<sub>2</sub>Ph), and followed the reaction by UV-visible spectrophotometry in *n*-decane, dioxane, methanol and dioxane:methanol (1:1) solvent systems at various temperatures. They found that the formation of the aminocarbene complexes [Cr(CO)<sub>5</sub>{C(NHR)Ph}] follows the fourth-order rate law:

$$\frac{d[\text{aminocarbene}]}{dt} = k_A [\text{alkoxy carbene}] [\text{RNH}_2] [\text{HX}] [\text{Y}]$$



More recent kinetic studies on aminolysis of alkoxy-carbene complexes are included in the work of Bernasconi and Ali<sup>[3;20-22]</sup>. They found that the second-order rate constant ( $k_A$ ,  $m^{-1}s^{-1}$ ) increases with amine concentration, giving a linear dependence with a tendency towards levelling off at higher amine concentration. They proposed that the reaction undergoes base catalysis, with a mechanism very similar to those for ester reactions, involving a nucleophilic addition of amine to the substrate to yield a zwitterionic tetrahedral intermediate in the first step, followed by deprotonation. In the third step, the intermediate is converted to product by water and/or conjugate acid of the base.

### 5.1.2 Focus of this study

The aminolysis reaction of the ethoxycarbene complexes synthesized in Chapter 2, with the amines ammonia and propylamine, was investigated.

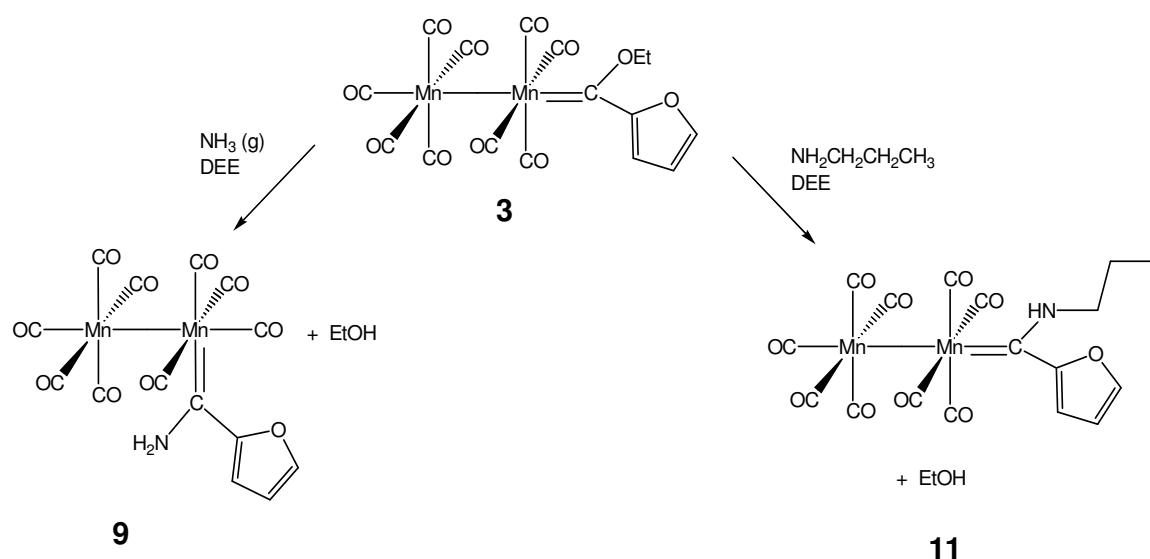


**Figure 5.1** Reactions to be studied kinetically via UV-visible spectrophotometry

The aim was to elucidate the reaction mechanism of the nucleophilic substitution of -OEt by -NHR in the reaction solvent diethyl ether, as well as to identify intermediates formed, which could then possibly explain the axial-equatorial isomerization observed during reaction with the very small amine  $\text{NH}_3$ .

## 5.2 Electronic Spectra

Three intense bands are present on the UV-spectrum of thiophene in the gas phase at 240 nm, 207 nm and 188 nm. Two bands, at 215 nm and 231 nm, are observed on the spectrum of thiophene in solution<sup>[23]</sup>. Substituents on the ring have an influence on the position of these bands, depending on the ring position of the substituent. Furan also exhibits two bands in solvent dichloromethane (232 nm, 283 nm) and hexane (244 nm, 277 nm)<sup>[24]</sup>, but only one band is observed in ethanol (208 nm)<sup>[25]</sup>.

The UV-visible spectra of the complexes **2**, **3**, **8** - **11** were recorded in diethyl ether, the solvent employed in the aminolysis reaction. The electronic data of these complexes are summarized in Table 5.1, and the electronic spectrum of complex **3** is presented in Figure 5.2.

**Table 5.1** UV-visible data of complexes **2**, **3**, **8** - **11** recorded in diethyl ether

Complex	Colour	Ligand $\pi$ - $\pi^*$ transition ( $\lambda$ , nm)	Metal-ligand transition ( $\lambda$ , nm)
<b>2</b>	orange-red	276, 350	414
<b>3</b>	orange-red	300, 350	396
<b>8</b>	yellow-orange	308, 346	436
<b>9</b>	yellow-orange	292, 346	442
<b>10</b>	yellow-orange	278, 354	436
<b>11</b>	yellow-orange	282, 354	442

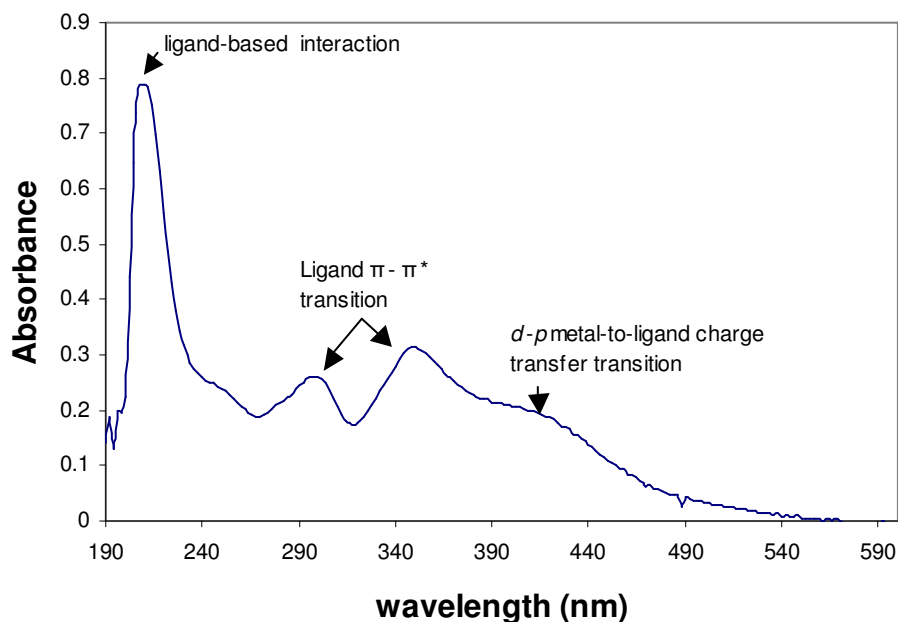


**Figure 5.2** UV-spectrum of **3**

All complexes exhibit strong ligand-based absorption bands between 242 - 253 nm. Two intense characteristic absorption bands with  $\lambda_{\text{max}}$  in the range 276 - 354 nm are the thiophene/furan-based  $\pi$ - $\pi^*$  transitions. Coordination to metal fragments shift these bands to higher wavelengths, indicating interaction of the metal carbene  $\pi$ -system with that of the heteroaryl substituent<sup>[24;26]</sup>. The energies of the  $\pi$ - $\pi^*$  transitions in the heteroarenes are reduced.

The absorption band at lower energy is assigned to a  $d$ - $p$  metal-to-ligand charge transfer (MLCT) transition<sup>[27]</sup>. The metal donates electrons to the empty  $p$ -orbital of the carbene carbon in the excited state whilst the heteroatom bonded to the carbene carbon atom acts as a  $\pi$ -donor towards the metal in the ground state (Figure 5.3). Since the colours of these complexes are characteristic to the number of metal moieties coordinated to the ligand the values of this transition are very similar for different monocarbene complexes of Cr, W and Mo of an orange-red colour<sup>[24;26]</sup>, with absorption energy ranging from 460 - 493 nm in these complexes. In the case of the dimanganese monocarbene complexes synthesized, these bands are

slightly overlapped by the  $\pi$ - $\pi^*$  transition bands, but can be distinguished as distinct shoulders.

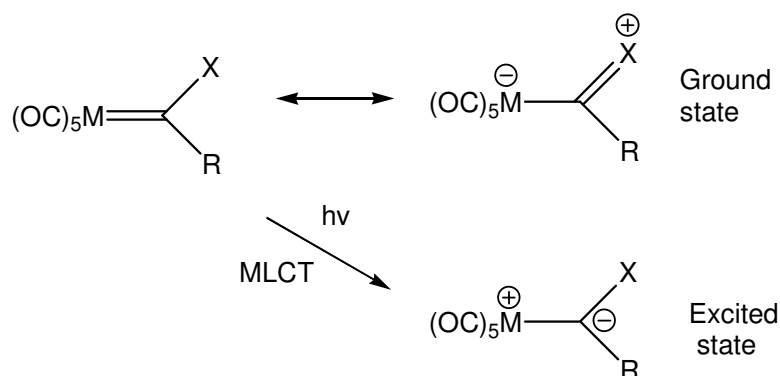


**Figure 5.3** Ground and excited states in Fischer carbene complexes

### 5.3 Kinetic Investigation

The aminolysis reaction of **2** converted into **8**, **10** and **3** into **9**, **11** can be studied by spectroscopic techniques, as conversions are associated with major spectral changes. In essence, no differences in the general kinetic behaviour of **2** and **3** were observed. Since the same reaction occurs for both complexes **2** and **3**, our kinetic investigations focused on **3** and its converted products. Aminolysis reactions of **3** were studied, employing two different amines: ammonia, which yields equatorially substituted **9**, and propylamine, which yields **11**, an axially substituted complex.

The UV-vis spectrum of **3** in diethyl ether display maxima at 300, 350 and 396 nm, and minima at 270, 318 and 384 nm. For **9** and **11**, the maxima are 292, 346, 442 nm and 282, 354, 442 nm respectively, while the minima are 272, 318, 408 nm and 286, 320, 412 nm respectively. The nucleophilic substitution of the ethoxy group by an amine group during the conversion of **3** into **9**, **11** is accompanied by characteristic changes in the spectra, as indicated by a decrease in the intensity of the band at 350 nm, shift of the shoulder maximum at 396 nm to 442 nm, and the shift of the maximum at 300 nm to 292 nm and 282 nm for **9** and **11**, respectively.

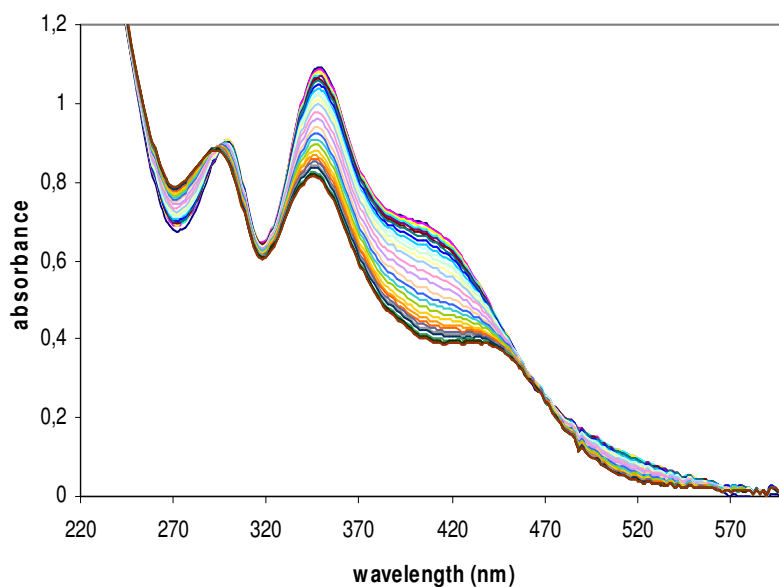


**Figure 5.4** Repetitive scan spectra recorded for the conversion of **3** to **9** at 25°C, experimental conditions  $[3] = 5.70 \times 10^{-5} \text{M}$ ,  $t_{\text{total}} = 10200 \text{ s}$

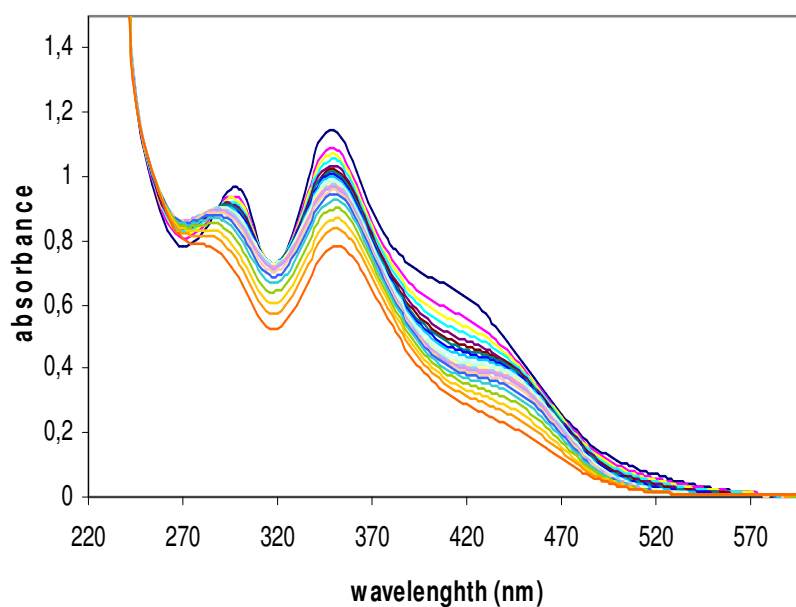


**Figure 5.5** Repetitive scan spectra recorded for the conversion of **3** to **11** at 25°C, experimental conditions  $[3] = 4.50 \times 10^{-5} \text{M}$ ,  $t_{\text{total}} = 14400 \text{ s}$

The progress of the reaction was therefore monitored by the increase and decrease of the  $\pi$ - $\pi^*$  ligand transitions and MLCT bands over the range 220 - 600 nm. The repetitive scan spectra recorded for the conversion of **3** to **9** is shown in Figure 5.4, and in Figure 5.5 for the propylamino-analogue **11**.

The spectra exhibit two initial isosbestic points at 288 nm and 452 nm, and 286 nm and 458 nm for **3** converted to **9** and **11** respectively. No calculations of the isosbestic points were done, due to the decomposition that occurred after approximately 4000 s, causing a drift of the isosbestic points.

For both reactions studied, the concentration of the amine reagent was always in great excess compared to that of the parent ethoxycarbene reagent, so that the kinetic experiments were conducted under pseudo-first order conditions, with the carbene complex as the minor component at 25 °C. Typical substrate concentrations were  $(3.0 - 6.0) \times 10^{-5} \text{ mol.L}^{-1}$  while the amine concentrations varied for  $[\text{NH}_3] = (1.08 - 10.8) \times 10^{-2} \text{ mol.L}^{-1}$  and  $[\text{propylamine}] = (3.04 - 12.20) \times 10^{-2} \text{ mol.L}^{-1}$ . The pseudo-first-order rate constants ( $k_{obs}$ ,  $\text{s}^{-1}$ ) were obtained by fitting the kinetic absorbance-time traces (measured at wavelengths 348 nm for **9** and 354 nm for **11**) with a suitable computer-fit program (See Section 6.2.6 in Chapter 6).

Table 5.2 lists data obtained for the reaction of **3** converted to **9** in ether at different concentrations of ammonia, and for the analogous conversion into **11** at different concentrations of propylamine. The values listed in Table 5.2 are the average values obtained of at least four kinetic traces, but the irreproducibility of these measurements, caused by the decomposition of the complexes, rendered fitting of the  $k_{obs}$  vs [amine] graphs difficult.

In both cases, the observed pseudo-first order rate constants,  $k_{obs}$ , showed a non-linear dependence on amine concentration (Figure 5.6 and 5.7), indicating a change in the order of the reaction from second- or mixed order to first-order in amine concentration<sup>[20]</sup>. When plotting the values of  $k_{obs}$  obtained for these reactions against  $[\text{amine}]^2$ , a seemingly linear dependence was



obtained (Figure 5.8, 5.9). This indicated that  $k_{obs}$  is the second-order rate constant. In all graphs, a zero point was added for aiding the fitting of the plotted data points.

**Table 5.2** Kinetic data for the influence of the concentration of the amines on the aminolysis reaction in diethyl ether at 25 °C.

Conversion of <b>3</b> to <b>9</b> [ <b>3</b> ] = $5.70 \times 10^{-5} \text{M}$		Conversion of <b>3</b> to <b>11</b> [ <b>3</b> ] = $4.50 \times 10^{-5} \text{M}$	
[NH <sub>3</sub> ] (mol.L <sup>-1</sup> )	$k_{obs}$ (s <sup>-1</sup> )	[propylamine] (mol.L <sup>-1</sup> )	$k_{obs}$ (s <sup>-1</sup> )
$1.08 \times 10^{-2}$	$3.26 \times 10^{-4}$	$3.04 \times 10^{-2}$	$5.79 \times 10^{-4}$
$2.16 \times 10^{-2}$	$6.89 \times 10^{-4}$	$6.08 \times 10^{-2}$	$2.35 \times 10^{-3}$
$5.40 \times 10^{-2}$	$2.09 \times 10^{-3}$	$9.12 \times 10^{-2}$	$5.98 \times 10^{-3}$
$7.20 \times 10^{-2}$	$6.92 \times 10^{-3}$	$1.22 \times 10^{-1}$	$1.18 \times 10^{-2}$
$8.64 \times 10^{-2}$	$1.00 \times 10^{-2}$	-	-
$1.08 \times 10^{-1}$	$2.10 \times 10^{-2}$	-	-

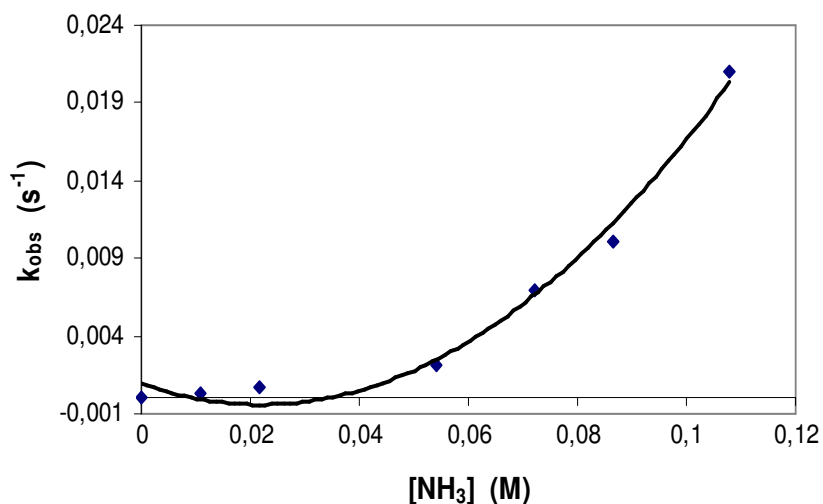


**Figure 5.6** Plot of  $k_{obs}$  vs [NH<sub>3</sub>] for the reaction between ammonia and **3** in diethyl ether at 25 °C

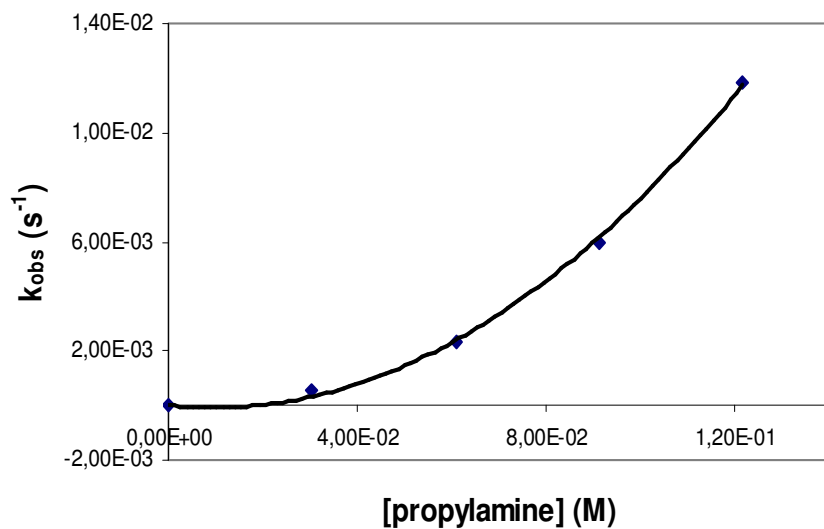


**Figure 5.7** Plot of  $k_{obs}$  vs [propylamine] for the reaction between propylamine and **3** in diethyl ether at 25 °C

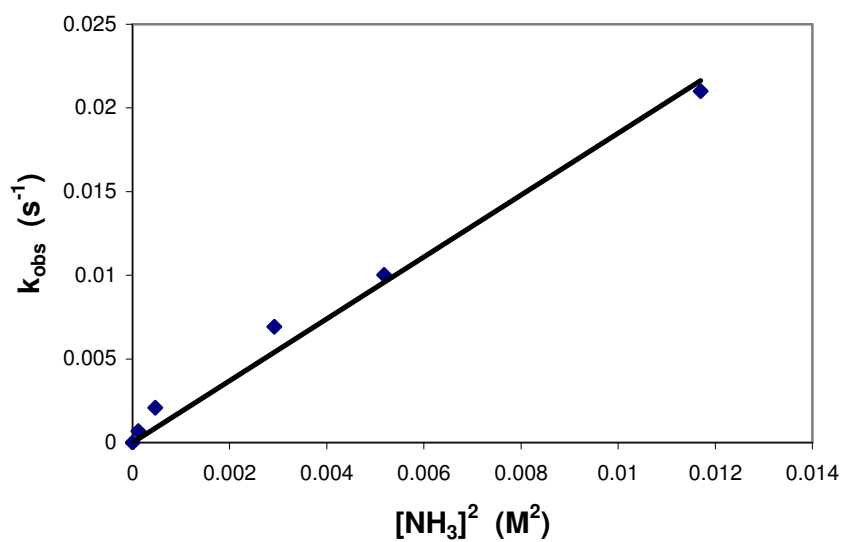


**Figure 5.8** Plot of  $k_{obs}$  vs  $[NH_3]^2$  for the reaction between ammonia and **3** in diethyl ether at 25 °C

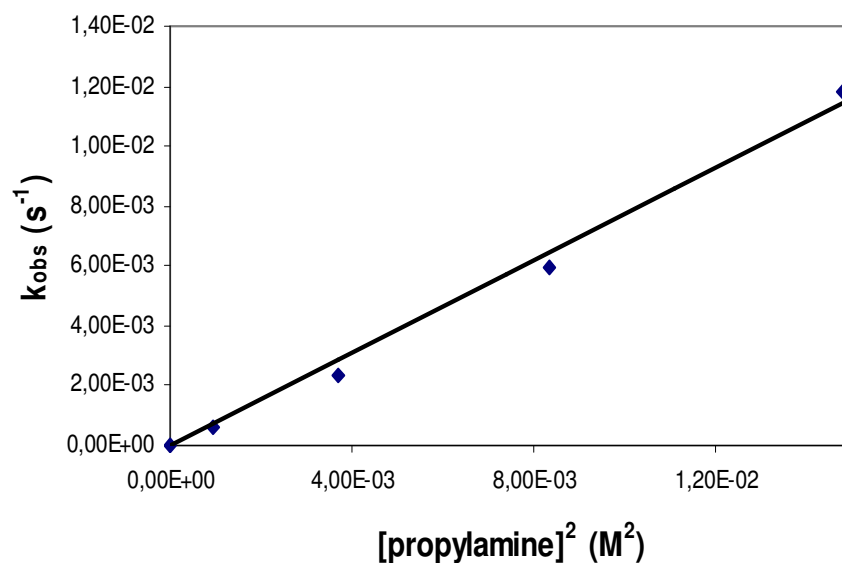


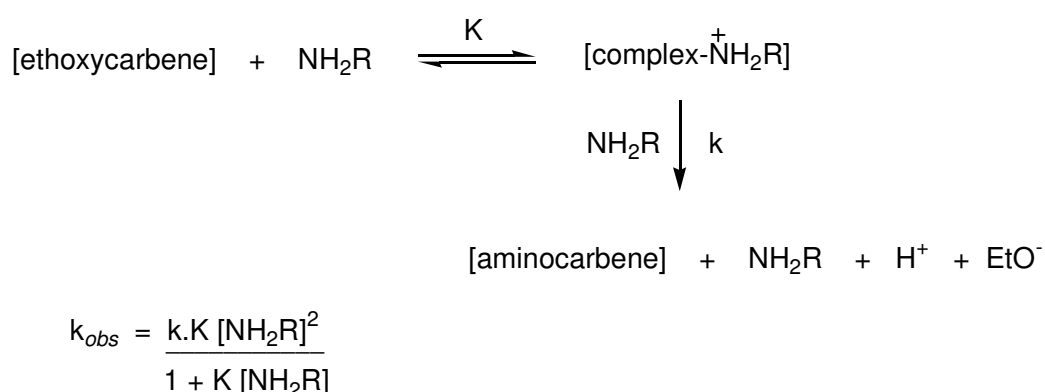
**Figure 5.9** Plot of  $k_{obs}$  vs  $[\text{propylamine}]^2$  for the reaction between propylamine and **3** in diethyl ether at 25 °C

## 5.4 Conclusions

These results would indicate a second-order reaction, involving at least two amine molecules during the aminolysis reaction. It was not possible to study the temperature or pressure dependence of these reactions, due to experimental difficulties associated with diethyl ether as solvent. The low boiling point and vapour pressure of ether, as well as its reaction with the plastic chambers within the high-pressure stopped-flow spectrophotometer, rendered the results obtained irreproducible. Another very important contributing factor to the irreproducibility of the results is the competing decomposition of the carbene complexes, as seen in Figure 5.4, 5.5. This meant that neither the Arrhenius activation energy, nor the reaction activation enthalpy or entropy could be calculated.

No significant differences were observed for the reactions of **3** with ammonia, compared with propylamine, except for the larger  $k_{obs}$  values determined for the reaction with ammonia. Therefore, no absolute information could be obtained about the axial-equatorial isomerisation. The two cases appear similar, which could mean that the axial-to-equatorial conversion only occurs later, to yield the thermodynamically favoured product, and not during the initial aminolysis reaction. Another indication that this might be a possibility is seen by the mixture of isomers seen in the NMR spectra of the manganese aminocarbene complexes (Chapter 4).

A probable reaction route could be postulated, as illustrated in Scheme 5.2, where at high concentrations of amine,  $k_{obs} = k[\text{amine}]$ , and at low concentrations of amine,  $k_{obs} = k.K[\text{amine}]^2$ .



**Scheme 5.2** Postulated reaction mechanism

No further information about intermediates could be deduced, but the results obtained can be explained by the mechanisms proposed by Werner, and Bernasconi and Ali discussed in Section 5.1. The second-order rate constant determined agrees with the findings of Ali<sup>[20]</sup> but not with the results of Werner<sup>[9]</sup>, where the aminolysis reaction of  $[\text{Cr}(\text{CO})_5\{\text{C}(\text{OMe})\text{Ph}\}]$  follows the fourth-order rate law.

## 5.5 References

1. K.H. Dötz, H. Fischer, P. Hofmann, F.R. Kreissl, U. Schubert, K. Weiss, *Transition Metal Carbene Complexes*, VCH Verlag Chemie, Weinheim **1983**.
2. R. Aumann, P. Hinterding, C. Kruger, R. Goddard, *J. Organomet. Chem.* 459, **1993**, 145.
3. C.F. Bernasconi, F.X. Flores, K.W. Kittredge, *J. Am. Chem. Soc.* 119, **1997**, 2103.
4. C.F. Bernasconi, L. Garcia-Rio, *J. Am. Chem. Soc.* 122, **2000**, 3821.
5. U. Klabunde, E.O. Fischer, *J. Am. Chem. Soc.* 89, **1967**, 7141.
6. J.A. Connor, E.O. Fischer, *J. Chem. Soc. A*, **1969**, 578.
7. E.O. Fischer, B. Heckl, H. Werner, *J. Organomet. Chem.* 28, **1971**, 359.
8. C.F. Bernasconi, M.W. Stronach, *J. Am. Chem. Soc.* 115, **1993**, 1341.
9. H. Werner, E.O. Fischer, B. Heckl, C.G. Kreiter, *J. Organomet. Chem.* 28, **1971**, 367.
10. E.O. Fischer, M. Leupold, C.G. Kreiter, J. Müller, *Chem. Ber.* 105, **1972**, 150.
11. C.T. Lam, C.V. Senoff, J.E.H. Ward, *J. Organomet. Chem.* 70, **1974**, 273.
12. R. Aumann, J. Schröder, *Chem. Ber.* 123, **1990**, 2053.
13. C.F. Bernasconi, K.W. Kittredge, F.X. Flores, *J. Am. Chem. Soc.* 121, **1999**, 6630.
14. E.O. Fischer, S. Riedmüller, *Chem. Ber.* 109, **1976**, 3358.
15. T.J. Burkhardt, C.P. Casey, *J. Am. Chem. Soc.* 95, **1973**, 5833.
16. C.P. Casey, T.J. Burkhardt, C.A. Bunnell, J.C. Calabrese, *J. Am. Chem. Soc.* 99, **1977**, 2127.
17. E.O. Fischer, G. Kreis, F.R. Kreissl, C.G. Kreiter, J. Muller, *Chem. Ber.* 106, **1973**, 3910.
18. C.P. Casey, W.P. Brunsvold, *Inorg. Chem.* 16, **1977**, 391.

19. R.A. Bell, M.H. Chrisholm, D.A. Couch, L.A. Rankel, *Inorg. Chem.* 16, **1977**, 677.
20. M. Ali, *New J. Chem.* 27, **2003**, 349.
21. C.F. Bernasconi, M. Ali, *J. Am. Chem. Soc.* 121, **1999**, 11384.
22. M. Ali, D. Maiti, *J. Organomet. Chem.* 689, **2004**, 3520.
23. Y. Mazaki, K. Kobayashi, *Tetrahedron Lett.* 30, **1989**, 3315.
24. C. Crause, *Synthesis and Application of Carbene Complexes with Heteroaromatic Substituents*, University of Pretoria, **2004**.
25. R.P. Kreher, *Houben-Weyl Methoden Der Organischen Chemie*, 1st ed. Stuttgart, New York **1994**, 328.
26. M. Landman, *Synthesis of Metal Complexes with Thiophene Ligands*, University of Pretoria, **2000**.
27. D.F. Shriver, P.W. Atkins, *Inorganic Chemistry*, 3rd ed. Oxford University Press, Oxford **1999**, 437.